CASE FILE
COPY

NACA RM A55F29

NACA

RESEARCH MEMORANDUM

FUSELAGE SIDE INLETS - A STUDY OF SOME FACTORS

AFFECTING THEIR PERFORMANCE AND A

COMPARISON WITH NOSE INLETS

By Emmet A. Mossman, Frank A. Pfyl, and
Frank A. Lazzeroni

Ames Aeronautical Laboratory
Moffett Field, Calif.

NATIONAL ADVISORY COMMITTEE
FOR AERONAUTICS

WASHINGTON
April 2, 1956
Declassified January 12, 1961

NACA RM A55F29

NATIONAL ADVISORY COMMITTEE FOR AERONAUTICS

RESEARCH MEMORANDUM

FUSELAGE SIDE INLETS - A STUDY OF SOME FACTORS

AFFECTING THEIR PERFORMANCE AND A

COMPARISON WITH NOSE INLETS[1]

By Emmet A. Mossman, Frank A. Pfyl, and
Frank A. Lazzeroni

SUMMARY

This report first notes briefly certain basic principles affecting the performance of side-inlet air-induction systems. Following this discussion, the performance of several fuselage side inlets is examined, and comparison is made with nose inlets. Methods for improving the performance of both side inlets and nose inlets are reviewed, including boundary-layer control on the compression surfaces, revised geometry to provide a circular side inlet, and an internal-compression inlet having low external drag.

A procedure is outlined for analyzing inlet flow instability from a statistical point of view in which the flow is treated as a stationary random function of time. It is suggested that the root-mean-square amplitude of the pressure fluctuations be related to jet-engine performance and that the method can prove useful for correlating inlet instability obtained from wind-tunnel models with results from flight tests.

INTRODUCTION

In the design of an air-induction system to supply air efficiently to an engine placed in an airframe, consideration must be given to the somewhat diverse fields of aerodynamics and thermodynamics. Airplane range, and variously defined airplane efficiencies, can be shown to be functions of the lift-to-drag ratio and the propulsive efficiency. Generally speaking, the lift-to-drag ratio is considered to be in the province of the

[1]This report is substantially the same as a paper presented at an Institute of the Aeronautical Sciences Specialist Meeting, on March 21, 1955, in Los Angeles, California.

aerodynamicist and the propulsive efficiency to be in the province of the thermodynamicist. The induction-system design involves both aerodynamics and thermodynamics; it can have a major influence on the drag of the airplane, and it affects the engine performance through deceleration of the induction air. It is the combination of these factors that makes induction-system design so vital to airplane performance.

As the aerodynamicist well knows, there is a divergence of opinion as to where the engine should be placed in any given design. This is especially true with a multiengine interceptor or fighter aircraft. It is beyond the scope of this paper to discuss relative merits of nacelles or pod installations as opposed to engine-fuselage arrangements. The aerodynamic and thermodynamic factors which should influence the design of an air-induction system are in the main known, but the information regarding them is diffused in the mass of literature dealing with subjects other than air-induction systems. In some cases the necessary research has not as yet been performed. It is the purpose of the present paper to discuss some of the aerodynamic factors which influence the performance of fuselage side inlets in the supersonic speed range up to a Mach number of about 2.0.

NOTATION

a maximum total amplitude of the pressure pulsation, lb/sq ft

C_D drag coefficient, $\dfrac{D}{qS}$

d diameter of body, ft

D net drag (measured drag minus the internal drag), lb

f frequency, cps

F_n net thrust, lb

$G(f)$ spectral density, $\dfrac{(\text{lb/ft}^2)^2}{\sec}$

h height of boundary-layer removal duct, ft

l length of body, ft

m mass flow through inlet, slugs/sec

$\dfrac{m_1}{m_\infty}$ ratio of the mass flow through the inlet to the mass flow at free-stream conditions passing through an area equal to the inlet entrance area

M   Mach number

p   static pressure, lb/sq ft

$\bar{p}$ root-mean-square static pressure, lb/sq ft

p_t total pressure, lb/sq ft

q   dynamic pressure, lb/sq ft

S   reference area, sq ft

x   longitudinal distance, ft

α angle of attack, deg

δ boundary-layer thickness, ft

θ cone or wedge angle, deg

λ cowl lip angle, deg

Subscripts

∞ free-stream condition

1   inlet station

BL   boundary-layer duct

c   compressor station

isen   isentropic

s   surface

t   total

DISCUSSION

Primary Principles

Performance improvements of air-induction systems can be expected to come from the application of certain fundamental aerodynamic principles related to the potential and viscous flow field of the body into which the

inlet is located, supersonic wave drag concepts, and boundary-layer shock-
wave interaction effects. Before discussing the detailed results of recent
research studies on side inlets, it would be well to review briefly these
primary principles.

For nose inlets, the air flow up to the entrance is uniform. However,
with side inlets the potential flow field of the fuselage at the inlet is
nonuniform, there being both longitudinal and radial velocity gradients.
The potential flow field of the fuselage, therefore, should influence to
a great extent the choice of the inlet location. Figure 1, obtained from
reference 1, shows a typical Mach number distribution along a fuselage
nose. In the selection of a fuselage nose shape, the location of the
inlet as well as the drag of the nose should be considered. If possible,
advantage should be taken of the compression afforded by the nose. The
inlet location should be selected so that the local Mach number is either
below or near the free-stream value. For symmetrical fuselages, the known
theoretical methods of computing the Mach number or pressure distribution
give very good results; the first-order linearized theory (refs. 2 and 3)
and the second-order theory (ref. 4) are adequate in this respect. For
asymmetrical bodies a few cases have been treated in the literature
(ref. 5).

Thus far only the potential flow field of the body at 0° angle of
attack has been considered. Viscous crossflow effects become important as
the angle of attack of the fuselage is changed. These effects are well
known and have been pointed out in references 6 and 7. A sketch represent-
ing the physical process of viscous crossflow is also shown in figure 1.
Here it is seen that as the angle of attack is increased, differences in
the pressure field around the circumference of the body cause the boundary
layer to flow into the top region, forming two lobes of low-energy air. As
the angle of attack is increased further, these lobes form vortices.
Extensive investigations of inlets at various circumferential locations on
bodies of revolution have been made at both the Lewis and Langley labora-
tories (refs. 8 and 9). These tests show that inlets on the bottom and
sides of the fuselage can have satisfactory characteristics; but difficul-
ties have been experienced with the upper locations, especially with regard
to the pressure recovery. However, some recent research has shown that
with the inlet on the top, the effect of the vortices can be minimized by
means of splitter plates and, consequently, the angle-of-attack effects
need not be as adverse as those measured originally (ref. 10). When inlets
are located on the sides of the fuselage, the local stream angle is greater
than the angle of attack of the body. This effect decreases rapidly as the
inlets are moved away from the fuselage.

In an examination of the basic concepts related to side inlets,
mention should be made of applications of the "area" rule; that is, the
estimation of wave drag from the longitudinal area distribution of a body
(ref. 11). The literature indicates that, at the present time, it is not
known how to apply the area rule to side-inlet air-induction systems.

Tests on nose inlets, however, have shown that the area rule can be used for these designs. The wave drag of nose inlets operating at maximum mass flow has been predicted by the use of equivalent closed-body concepts (ref. 12). These nose inlet studies made at the Langley laboratory have indicated that the accuracy of the area-rule applications to nose inlets on slender bodies depends upon the ratio of the diameter of the inlet to the maximum diameter of the body. The accuracy appears to be good for ratios less than 0.3 to 0.4.

In a review of the factors which influence the performance of side inlets emphasis should be placed on shock-wave boundary-layer interaction. With side inlets the streamtube of induction air is contiguous to the fuselage surface, and the deceleration and compression of this air is accomplished by a shock-wave system which may impinge on the fuselage boundary layer. If the inlet is placed away from the fuselage, boundary-layer shock-wave interaction still occurs on the compression surfaces and may affect adversely the pressure recovery, air-flow stability, and drag of the inlet system. Schlieren studies of shock-wave boundary-layer interaction on probes in front of a blunt body (see, e.g., ref. 13) have indicated that for a shock wave of a given strength, the upstream disturbance is much less if the wave impinges on a turbulent boundary layer than if it interacts with a laminar or transitional boundary layer. It is believed that the photographic sequence shown on figure 2 illustrates these same effects for the case of air flow on the ramp of an inlet. At the top of the figure is shown an inlet operating at its maximum mass flow with the normal shock inside the inlet. As the mass flow is reduced, the normal shock moves in front of the inlet and interacts with the ramp boundary layer. The boundary layer is believed to be turbulent and the extent of the pressure disturbance which is transmitted upstream through the boundary layer is small, as indicated by the small wedge of separated air. With further reduction in the mass-flow ratio, the normal shock wave moves farther forward and finally interacts with a laminar or transitional portion of the boundary layer on the ramp. The upstream influence of the pressure disturbances is much greater, as can be seen in the region of separation extending to the very tip of the ramp. Accordingly, in the design of air-induction systems, interaction of the shock waves with laminar boundary layers should be avoided.

The influence of shock-wave boundary-layer interaction on air-induction performance appears to have been recognized by early investigators in the field of air induction. However, the importance of defining a satisfactory criterion for predicting the occurrence of shock-induced separation appears to have been overlooked. At the present time, the physical measurement of this interaction in which we are most interested is the pressure rise necessary to separate a boundary layer. Lange, in reference 14, reviewed in 1953 the known published information on the subject of the pressure rise which was then considered to be necessary to separate boundary layers. These and additional data are reviewed in figure 3. It is important to note that many diverse methods were used to

obtain the data, and that different criteria were used to determine the existence of separation. In the cases summarized by Lange, the pressure ratio for separation is obtained from the first peak pressure in the region of the wedge or the step. Schlieren observations of the bifurcation of a normal shock wave on the cone compression surfaces of nose-inlet models have been used by Nussdorfer as an indication of separation (ref. 15). Seddon used the surface pressures in the dead-air region behind a normal shock wave. At Mach numbers up to about 1.4, the pressure gradient was produced by a normal shock and subsonic diffusion between the shock system and the entry (ref. 16). Fage and Sargent made tests in which a normal shock wave produced the gradient necessary to separate the boundary layer, the separation being indicated from schlieren observations and pressure measurements (see ref. 17). The agreement between these methods is poor. The results are contrary to those reported by Bogdonoff and Kepler (ref. 17), who indicate no change in the separation pressure rise with Mach number. In the studies of boundary-layer shock-wave interaction previously cited, the pressure required to produce separation is taken to be that measured at the point of separation; however, recent unpublished information indicates that the required pressure rise is somewhat greater. In many practical installations it is not possible to design the ramp so that the pressure rise for separation will not be exceeded. If the separated flow can be made to reattach in these cases by use of boundary-layer control and other devices, the air-flow stability and pressure recovery can be improved. There would seem to be a need for new concepts relating to air-inlet design which take into account the separation criteria. It is clear, however, that the limits of these separation criteria are not well defined and that more research is indicated. The advancement of the inlet field depends to a large extent upon the research that will be done on this particular phase.

Performance of Side Inlets

The preceding primary principles provide a basis for anticipating improvements in side-inlet performance. It is not possible, however, always to take full advantage of the aerodynamic gains afforded by these concepts. In many cases structural or weight considerations may preclude certain inlet locations. In addition, many of the fundamental principles are still somewhat rudimentary, as is the case of the application of the area rule to air-induction design. Keeping in mind these and similar limitations to the application of the primary principles, let us consider next the performance of some actual side-inlet installations. Where possible, comparisons are made with nose-inlet installations. Figure 4 shows the pressure recovery of normal-shock side inlets as a function of free-stream Mach number. The pressure recovery at 95 percent of the maximum mass-flow ratio has been selected arbitrarily for comparison of the various inlets. The solid line curves present data on designs for various airplanes or missiles which were tested in wind tunnels as a part of developmental research programs (refs. 18 to 21). The dashed curves give

results of laboratory experiments on more idealized experimental models
and also on pitot nose-inlet installations (refs. 22 to 25). Normal-
shock pressure recovery is shown also on the figure. Except for one case,
there is an increment of about 0.04 between the side-inlet and nose-inlet
induction systems at the higher Mach numbers. The exception is a circular
side inlet (ref. 21) which exhibits considerably higher pressure recovery
than the conventional type, its value approximating that for the nose
inlets. Additional data will be given on this inlet later in the paper.
Generally, it is realized that normal-shock inlets inflict severe perform-
ance penalties if they are used at Mach numbers above about 1.4.

The known recent pressure-recovery data on oblique-shock scoop inlets
as applied to practical airplane models is summarized in figure 5 (refs. 21
and 26 to 28). There are little data on comparable nose inlets with ramps
or wedges. From a review of the literature, it becomes evident that there
are more side-inlet designs with wedges than with cones. However, with
nose inlets or nacelles, the research on cone compression surfaces pre-
dominates. The pressure recovery of these practical side inlets is
dependent on the design Mach number. The rapid dropoff in pressure
recovery occurs at Mach numbers above that for which the oblique shock
falls inside the inlet. Very good pressure recovery has been obtained with
some of the designs at Mach numbers less than about 1.5. At the higher
Mach numbers, difficulties have been encountered in reaching the values
of the pressure recoveries obtained with the best nose inlets with external
compression surfaces. A two-angle ramp has obtained the highest pressure
recovery ($p_{t_c}/p_{t_\infty} = 0.87$ at $M_\infty = 2.0$), although it should be noted that
the stable mass-flow-ratio range was not large for this particular inlet.

Very little data exist from which a direct assessment can be made of
the penalty in pressure recovery resulting from the placement of oblique-
shock inlets on the side of a fuselage. Two comparisons have been derived
from various published reports: One for an inlet design having a wedge-
compression surface; the other for inlets having cone-compression surfaces.
Figure 6 compares the pressure recovery of a nose inlet with a 14° wedge
with that of the same inlet placed on the fuselage (refs. 29 and 30). The
decrease in pressure recovery due to placing the inlet on the fuselage is
0 to 6 percent, depending on the Mach number. Comparison of various coni-
cal nose inlets with a half-cone inlet mounted on a flat plate (ref. 31)
and a half-cone inlet on several fuselages is shown in figure 7. Since a
conical nose inlet having a shape similar to the half-cone inlets was not
tested, a pressure-recovery range obtained from several recent conical
nose-inlet studies has been included on the figure (refs. 32 to 36). The
data presented in figure 7 show progressive decreases in pressure recovery
from the conical nose inlet to the half-cone inlet on the flat plate to
the half-cone inlet on the various fuselages.

The differences in the pressure recovery of nose inlets and the side inlets are due to the distortion of the potential flow field in the region of the inlet, to dissimilarities in the internal ducting, and to the viscous boundary layer of the fuselage on which the inlets are placed. The data on the two figures previously mentioned (figs. 6 and 7) are for boundary-layer control systems which were considered well designed. The magnitude of the decrease in pressure recovery of a side inlet as compared to a nose inlet can be much larger, depending to a great extent on the boundary-layer control system that is used.

Four boundary-layer control systems for side inlets which have been investigated are shown in figure 8. The suction or scoop type shown at the top of the figure takes the fuselage boundary layer into the fuselage. The diverter utilizes a wedge underneath the inlet to deflect the fuselage boundary layer as it passes underneath the compression surface and along the body. When a portion of the fuselage boundary layer can be put to some useful purpose, combinations of the suction and diverter systems are employed. A lesser amount of research, some at the Ames laboratory and some by the Royal Aircraft Establishment in Great Britain, has been done on the fourth type which removes only the low-energy portion of the fuselage boundary layer through a porous surface or through slots.

Before examining the characteristics of these boundary-layer control systems for supersonic inlets, let us consider first how they affect the flow into the inlet. That the boundary-layer control system can have a large influence on the flow field in front of the inlet is illustrated in the schlieren photographs of figures 9 and 10. These figures illustrate the effect of the boundary-layer diverter. Figure 9(a) shows the severe disturbances propagated upstream of a normal-shock inlet by a blunt 130° wedge. When the wedge angle was reduced to 65° (fig. 9(b)) and an indentation in front of the inlet was removed, the magnitude of the disturbances was greatly reduced, but not completely eliminated. Figure 10 shows how the oblique-shock system in front of a ramp-type inlet is altered by changes to the diverter angle of a combination of a diverter and suction system. In figure 10(a) the diverter wedge angle is about 40°. Although the schlieren photographs are not too clear, close examination shows that reducing the wedge angle to approximately 20° (fig. 10(b)) in the front portion of the diverter eliminated the disturbances. Piercy and Johnson in references 31, 37, and 38 have shown that wedge-type diverters yield inlet total-pressure recoveries comparable to the suction type, provided that small wedge angles are used and that the apex of the diverter wedge is downstream of the apex of the compression surface in front of the inlet. The penalty in pressure recovery incurred by placing the inlet in the fuselage boundary layer is shown in figure 11. Pressure recovery of several inlets is plotted as a function of h/δ, where h is the height of the boundary-layer control inlet above the fuselage and δ is the boundary-layer thickness. For the suction-type inlets, the mass flow through the boundary-layer removal system is the maximum used in the tests. It can be seen that diverter systems are more sensitive to placement in the

fuselage boundary layer than are suction systems. Although the inlet pressure recovery is increased as the inlet is moved out of the boundary layer of the fuselage, the drag of the airplane or missile is also increased.

The drag contributed by various boundary-layer control systems applied to airplane, missile, and research models is summarized in figure 12 (refs. 9 and 39). Basing the drag coefficients on the capture area of the boundary-layer control system, which has been done in this figure, should put the dissimilar configurations on a comparable basis, to first-order accuracy. The drag of the diverter is defined as the drag of the inlet-fuselage combination with diverter, minus the drag of the inlet-fuselage combination without the diverter (i.e., with the inlet placed contiguous to the fuselage and the inlet area increased by an amount equal to the area of the diverter system). For a ratio of capture area to wing area typical of four recent interceptors, these drag coefficients for the diverter systems represent from 3 to 10 percent of the total drag of an interceptor airplane. It can be seen that these forces are very large. The drag of the diverter system can be divided, roughly, into two components - the wedge pressure drag and the drag associated with viscous forces. An experimental breakdown of the drag is given in figure 13, which shows the magnitude of the two components (ref. 40). From this figure it is evident that large wedge angles should be avoided if the total diverter drag is to be kept small. The symbol in the figure is the total drag coefficient of a wedge-type diverter with a cusped shape; the data were obtained from model tests in the Ames 6- by 6-foot wind tunnel. If a straight wedge had been used, the diverter angle would have been 33°. The drag of this system was somewhat less than that for straight-sided wedges.

With one exception, the data shown in figure 12 were for inlets having diverter boundary-layer control systems. The drag was large for the one configuration which used a suction system. Subsonic tests at the Ames laboratory on an airplane in flight having a suction boundary-layer control system showed a drag-coefficient increment of 0.0015 even in the subsonic speed range (ref. 41). In both of these tests, the high drag seems to be associated with the design of the exit of the boundary-layer control duct. If there is no external disturbance due to exiting the air, the drag of the suction system can be computed as the loss of momentum of the boundary-layer air in passing through the ducting system. This momentum loss is inversely proportional to the pressure recovery in the boundary-layer scoop itself. A summary of the available information on the pressure recovery of the boundary-layer control duct is given in figure 14 (see refs. 31, 42, 43, 44, and 25). It can be seen from a comparison of the curves shown that in actual installations the recovery is much lower than the average pitot pressure through the boundary layer (ref. 45). The size of the internal boundary-layer duct necessary is also determined by the total-pressure recovery of the boundary-layer control system. This figure shows that in order to supply the same amount of air the ducting would have to be 1.5 to 2.0 times as large in these cases as

it would if the theoretical recovery were attained. Included for compari-
son purposes are the pressure recoveries measured beneath a sintered ramp
during model tests at the Ames laboratory. The amount of air removed was
from 2 to 2-1/2 percent of the inlet mass flow, which corresponds to about
15 percent of the boundary-layer air.

Methods for Increasing Side-Inlet Performance

Having summarized the pressure recovery and drag penalties associated
with many existing side-inlet installations, one may ask what methods are
being considered to increase their performance. Boundary-layer control on
the compression surfaces of the inlets has evidenced some promise. Fig-
ure 15 summarizes the results obtained on two separate models. These data
are for two side-inlet installations in which the ramp is approximately
one boundary-layer thickness away from the fuselage (ref. 27 and unpub-
lished data). The increase in pressure recovery is sizable, an increment
of 0.04 to 0.06 having been obtained with either porous-ramp surfaces or
a slot inside the inlet.

In an effort to improve side-inlet performance, configurations some-
what less conventional have been investigated. A circular side inlet and
a porous-ramp side inlet have been tested in the Ames 6- by 6-foot wind
tunnel. One of these, the circular inlet, is shown with a more conven-
tional ramp-type side inlet in figure 16. The porous-ramp side inlet,
which is not shown, is similar in shape to the ramp inlet shown in this
figure but has the porous compression surface contiguous with the fuselage,
thus having no diverter. Pressure recovery and drag of these three inlets
are compared in figure 17 at their matched operating condition, which cor-
responds to a range of mass-flow ratios from 0.77 to 0.95. The pressure
recovery of the circular inlet is not significantly different from that of
the ramp inlet with boundary-layer control when a diverter wedge is used.
At Mach numbers above 1.5, a curve of pressure recovery versus mass-flow
ratio shows the diverter inlet to have a higher pressure recovery at mass-
flow ratios greater than 0.85. It should be noted, however, that installa-
tion of a compression surface in the circular inlet could increase its
pressure recovery at the higher mass-flow ratios at Mach numbers above 1.5.
The porous-ramp trapezoidal inlet without a diverter, that is, with the
ramp next to the fuselage surface, has lower pressure recovery than the
other two inlets. The drag of the circular inlet is considerably less
than the drag of the conventional ramp inlet (see fig. 17). This drag
decrease amounts to about 6 percent of the total airplane drag. It is
believed that the drag reduction due to the circular inlet is associated
with the type of boundary-layer control system which offers less restraint
to the boundary-layer air as it flows rearward along the fuselage. The
drag of the porous-ramp inlet is less than that for the conventional ramp
inlet but greater than that for the circular inlet.

Schlieren observations of the flow field about the circular inlet and the ramp inlet, which has a trapezoidal entrance area, are shown in figures 18 and 19. These schlieren photographs were taken at a Mach number of 1.5 and show the shock pattern characteristics of these two inlets as the mass-flow ratio is reduced from a maximum. It is interesting to note the differences in the shock-wave boundary-layer interaction accompanying the normal shock wave in front of the inlets. There being no compression surface in front of the circular inlet, the normal shock is stronger than it is for the ramp inlet, and the upstream disturbances through the boundary layer give rise to an oblique shock wave. This oblique wave accounts for the high pressure recovery of the circular inlet at reduced mass-flow ratios.

A significant performance comparison of the three inlets tested involves a conversion of the drag force and pressure recovery into a single net propulsive force parameter (see fig. 20). The inlets and engine must also be compared at their actual operating points (at the operating or matched condition in which the air supplied by the inlet must be equal to the air required by the engine). For this analysis, a typical jet engine operating at sea level and 35,000 feet was assumed. The drag forces used in the computations are for the fuselage air-induction systems shown in the previous figure and do not include the drag of wing or tail surfaces. In the computations, the assumption is made that the drag is not affected by the small changes in the inlet area necessary to match the inlet-engine operation. The entrance area of the inlet simulated by the model during the tests was 4.2 square feet. In general, the circular inlet can be seen to have considerably better net propulsive force than either the conventional-ramp or porous-ramp inlets at supersonic speeds. Only small differences can be observed between the performance parameter for the conventional-ramp and porous-ramp inlets. It should be noted that at supersonic speeds the change in the net propulsive force parameter with inlet area (or with mass-flow ratio) is much less for the circular inlet than for either of the other two inlets, indicating a more favorable off-design performance for the circular inlet. Figure 20 shows that an entrance area of about 4.0 square feet, full scale, appears to be a good compromise, when the performance in the speed range from 0 to 1.5 is considered. Somewhat higher performance at supersonic speeds can be attained with an inlet area of 3.5 square feet. However, severe performance losses are incurred during subsonic operation. It should be remembered that the inlets which have been analyzed were designed primarily for operation at Mach numbers up to 1.5. When the inlets are designed for operation at higher Mach numbers, which change the external shape of the inlets, the net propulsive force parameter would be changed considerably at all speeds. The porous-ramp inlet which eliminated the diverter system was not entirely successful on this particular installation. Because only 2 to 2-1/2 percent of the inlet air was removed, the pressure recovery was not increased sufficiently to take advantage of the reduction in drag. It is possible that increases of perhaps 50 to 100 percent in the amount of air taken through the porous surface could result in better pressure

recovery for this type of inlet. It should be mentioned, however, that
the range of stable operation of the porous-ramp inlets without diverters
is less than that of the conventional-ramp inlets with diverters or the
circular inlet (which has the best stability characteristics).

An attempt is also being made to develop new types of inlets having
high performance, which can be used as either side inlets or in conjunc-
tion with nacelles. An inlet configuration which has been evolved
utilizes multishock compression, the compression occurring internally in
the inlet. The inlet that has been tested is shown in figure 21. Multi-
shock compression was selected so that the strength (or pressure rise) of
the initial shock would be below that necessary for separation. Internal
compression is used to eliminate the high drag, at Mach numbers greater
than 1.9, associated with multishock cone or wedge inlets having compres-
sion external to the inlet lips. The inlet is axially symmetric, and the
angles of the compression surfaces are low. A side-inlet installation
with this design might be similar to the circular inlet shown in figure 16.
To achieve high pressure recovery with an internal-compression inlet
requires that the contraction ratio approach that necessary for isentropic
recovery. Since a supersonic inlet will not start at these contraction
ratios, provision was made to vary the contraction ratio by making the
center cone movable. Starting in the supersonic speed range from $M = 1.6$
to $M = 2.1$ was accomplished by extending the cone. The inlets were
designed for maximum efficiency in the Mach number range from 1.9 to 2.1
when the center cone is set so that the apex is almost in the entrance
plane. The compression is as nearly as possible apportioned equally
between the compression surfaces. The circular inlet shape was selected
because it eliminated the corners and the two converging side walls of
rectangular internal-compression inlets. The angularity of the annular
compression surface was kept small to minimize the focusing of the oblique
shock waves at the center of the passage. These inlets have been tested
at Mach numbers of 1.9, 2.0, and 2.1. The pressure recovery measured is
shown on figure 22 together with the values from several other cone inlet
studies (refs. 23, 36, and 46 to 48). The pressure recovery of the
internal-compression inlet compares quite favorably with the cone inlets
(which have the highest pressure recovery obtained to date). The drag
resulting from external surfaces having such small deflection angles
(0° to 2°) is low. The lip angles of the cone inlets are from 10° to 25°,
which result in considerable drag penalties. Because of its low drag and
high pressure recovery, the internal-contraction inlet appears to show
considerable promise. The research is in a preliminary stage and more
complete investigation is planned.

Air-Flow Instability

The preceding comments have been restricted to those aspects of side-inlet performance which pertain to pressure recovery, drag, and net propulsive force. Little has been said concerning another factor in the design of induction systems which is equally as important as drag or pressure recovery, that is, inlet instability. With external-shock inlets, the instability is indicated by rapid flow pulsations which are usually encountered as the mass-flow ratio is reduced below its maximum. The following discussion of this problem includes a brief examination of the current theoretical views concerning inlet instability, a short summary of the effect of inlet instability on jet-engine performance, and a suggested method for analyzing and correlating inlet instability.

Several theories have been proposed to describe the mechanism of air-flow instability, or "buzz," and to determine the triggering force necessary for its start. These are given in references 49 through 53. None of these theories have been able to explain a majority of the cases where instability has occurred, and at least two different triggering forces, boundary-layer separation and a velocity discontinuity arising at the intersection of an oblique and a normal shock, are now known to incite buzz. Reports on most model experiments simply point out the mass-flow ratio at which the instability occurs. Little information has been given of the oscillating nature of the air flow, that is, measurements of the frequency and amplitude of the pressure pulsations that occur in the internal ducting.

Before discussing the effect of instability on engine performance, it is necessary to distinguish clearly between air-flow pulsations at the compressor inlet and air-flow distortion at the compressor inlet. Flow distortion has been considered a steady-state condition. The distribution of total pressure at the compressor has been the parameter most widely used to correlate distortion patterns with decreases in jet-engine performance. Inlet instability produces air-flow pulsations, resulting in nonsteady flow processes. Very little qualitative research, and no quantative studies have been made to determine a parameter suitable for correlating air-flow pulsations with jet-engine performance. A few attempts have been made to use the distribution of total pressure at the compressor inlet, the basis apparently being that certain of the engine manufacturers have required that the total pressure should not vary over

5 percent. If the problem is one of flow distortion then such a parameter
might be useful; however, it has no obvious connection with oscillating
flows.[2]

It has been shown, experimentally, by several investigators that air-
flow distortion at the compressor inlet can impair the performance of jet
engines, in some cases causing premature surging of the compressor. The
tests reported in reference 54 were made in an NACA altitude test chamber
at the Lewis laboratory on an axial-flow jet engine. The unequal flow
distribution in these tests was such as to cause failure of the turbine
under certain conditions. Before the failure, it also had the effect of
reducing the efficiency of the compressor and the turbine, so that the
thrust of the engine was reduced and the fuel consumption increased. Surg-
ing of jet-engine compressors also has been encountered during flight and,
in most cases, has been attributed to air-flow distortion. However, many
of these surges occurred under conditions where considerable flow unstead-
iness existed, the surging difficulties being encountered during take-off
and during high-speed climb and maneuvers, where separation from the inlet
lips was present. One experimental study has been made on a jet-engine
cone-inlet combination in the Lewis 8- by 6-foot wind tunnel which is
reported in reference 33. Although buzz occurred, it appeared to be less
severe with the engine installed and operating than it was with the engine
removed. The data presented do not include measurements of the amplitude
or frequency of the pressure fluctuations. It might be noted that buzz
for this type of inlet is triggered by a velocity discontinuity due to
the intersection of an oblique and a normal shock wave which comes in
contact with the inner lip surface of the cowl. In another case, for an
airplane in flight, the instability was started by separation induced by
boundary-layer shock-wave interaction. The occurrence of the instability,
which resulted in severe buffetting, agreed qualitatively with wind-tunnel
results, but detailed measurements were not made.

The few, and sometimes conflicting, experimental observations of the
effect of inlet instability on jet-engine performance direct attention to
the need for a more unified approach to this problem. It was noted that
records of the pulsating pressure in the induction system versus time, for
several wind-tunnel models, were similar to records obtained in the study
of velocity fluctuations in turbulent boundary layers. It was reasoned
that inlet buzz could be analyzed in the same manner that turbulent
boundary layers have been analyzed, that is, from a statistical point of
view. Treating the unsteady flow as a stationary random function of time
yields a method for constructing a more complete model of the flow

---

[2]It is impossible to obtain accurate and reliable data from a total-
pressure tube mounted in such flows. It has been shown by Goldstein, in
reference 55, that a total-pressure tube in an air stream with a fluctuat-
ing velocity will always indicate a pressure higher than the mean pressure.
There is also the unknown effect of damping by the length of tube that
connects the manometer with the total-pressure probe itself.

mechanism. By use of the concept of spectral density, it is possible to obtain the root-mean-square amplitude of the fluctuating pressure and to show the frequency range which contains the largest percentage of the turbulent energy (refs. 56 to 60). Figure 23 shows a typical pressure-time record that was obtained from one of the inlet models tested at the Ames laboratory. A schematic diagram of the method is outlined at the top of figure 24. The dynamic pressure cell which measures the oscillating pressures is mounted inside the inlet and the impulses from this cell are recorded onto a tape. The tape is then put through a wave analyzer which in turn plots the spectral density used in the analysis of the data. The spectral density derived from the magnetic tape as it is put through the wave analyzer is shown on the lower portion of the figure. These data are for a Mach number of 1.7 at a mass-flow ratio of 0.59. By integration of the total area beneath the curve of spectral density versus frequency, the root-mean-square amplitude of the pressure fluctuations can be obtained. This curve shows that the instability occurs between 10 and 450 cycles per second, with the energy being concentrated in two bands, one at 100 cycles and the other at 350 cycles. It was also determined from separate samples that the instability was a stationary random process.

The method employing the root-mean-square amplitude of the fluctuating pressure has been used in analyzing the data of two inlet models tested in the Ames 6- by 6-foot wind tunnel. Data for these two configurations are shown in figures 25 and 26. On the right of figures 25 and 26 are shown the maximum amplitude of the fluctuating pressure obtained from the pressure time records as a fraction of the free-stream total pressure. The curves on the left of figures 25 and 26 show the ratio of the root-mean-square fluctuating pressure (determined from spectral-density plots by the method just outlined) to the free-stream total pressure. For these two models, it can be seen that the ratio of the maximum amplitude may or may not be a smooth function of mass-flow ratio. However, in both cases the rms ratio of the fluctuating pressure is a smooth and continuous function of mass-flow ratio, its values increasing with increasing Mach number and with decreasing mass flow. It is interesting to note that the rms pressure amplitude does not increase suddenly, but increases smoothly as the mass-flow ratio is decreased. Schlieren observations of buzz, on the other hand, lead one to expect a sudden change of fluctuating pressure as the mass-flow ratio is decreased. It is believed that the rms amplitude, rather than the maximum amplitude of the pressure fluctuations are related to the jet-engine performance, and therefore the schlieren observations may be misleading. Use of this statistical approach should provide a

basis for analyzing the effects of pressure pulsations on jet engine performance and for correlating model and full-scale tests.

Ames Aeronautical Laboratory
    National Advisory Committee for Aeronautics
        Moffett Field, Calif., June 29, 1955

REFERENCES

1. Jorgensen, Leland H.: Correlation by the Hypersonic Similarity Rule
        of Pressure Distributions and Wave Drags for Minimum-Drag Nose
        Shapes at Zero Angle of Attack. NACA RM A53F12, 1953.

2. von Kármán, Theodore, and Moore, Norton Bartlett: Resistance of Slen-
        der Bodies Moving With Supersonic Velocities, With Special Reference
        to Projectiles. Trans. A.S.M.E. Dec. 15, 1932, pp. 303-310.

3. Ferri, Antonio: Elements of Aerodynamics of Supersonic Flows.
        Macmillan Co., New York, 1949.

4. Van Dyke, Milton D.: A Study of Second-Order Supersonic Flow Theory.
        NACA Rep. 1081, 1952.

5. Ferri, Antonio, Ness, Nathan, and Kaplita, Thaddeus T.: Supersonic
        Flow over Conical Bodies without Axial Symmetry. Jour. Aero. Sci.,
        vol. 20, no. 8, Aug. 1953, pp. 563-571.

6. Allen, H. Julian, and Perkins, Edward W.: Characteristics of Flow
        Over Inclined Bodies of Revolution. NACA RM A50L07, 1951.

7. Seiff, Alvin, et al: Aerodynamic Characteristics of Bodies at Super-
        sonic Speeds. A Collection of Three Papers. NACA RM A51J25, 1951.

8. Hasel, Lowell E.: The Performance of Conical Supersonic Inlets on
        Circular Fuselages. NACA RM L53I14a, 1953.

9. Valerino, Alfred S., Pennington, Donald B., and Vargo, Donald J.:
        Effect of Circumferential Location on Angle of Attack Performance
        of Twin Half-Conical Scoop-Type Inlets Mounted Symmetrically on
        the RM-10 Body of Revolution. NACA RM E53G09, 1953.

10. Kremzier, Emil J., and Campbell, Robert C.: Effect of Fuselage Fences
        on the Angle-of-Attack Supersonic Performance of a Top Inlet-Fuselage
        Combination. NACA RM E54J04, 1955.

11. Whitcomb, Richard T.: A Study of the Zero-Lift Drag-Rise Character-
      istics of Wing-Body Combinations Near the Speed of Sound. NACA
      RM L52H08, 1952.

12. Howell, Robert R.: A Method for Designing Low-Drag Nose-Inlet-Body
      Combinations for Operation at Moderate Supersonic Speeds. NACA
      RM L54I01a. 1954.

13. Daniels, Lloyd E., Capt., USAF, and Yoshihara, Hideo: Effects of the
      Upstream Influence of a Shock Wave at Supersonic Speeds in the
      Presence of a Separated Boundary Layer. WADC Tech. Rep. No. 54-31,
      Jan. 1954.

14. Lange, Roy H.: Present Status of Information Relative to the Pre-
      diction of Shock-Induced Boundary-Layer Separation. NACA TN 3065,
      1954.

15. Nussdorfer, Theodore J.: Some Observations of Shock-Induced Turbulent
      Separation on Supersonic Diffusers. NACA RM E51L26, 1954.

16. Holder, D. W., Pearcey, H. H., and Gadd, G. E.: The Interaction
      Between Shock Waves and Boundary Layers With a Note on the Effects
      of the Interaction on the Performance of Supersonic Intakes by
      J. Seddon. ARC Performance Sub-Committee 16,526, Feb. 2, 1954.

17. Bogdonoff, Seymour M., and Kepler, C. Edward: Separation of a Super-
      sonic Turbulent Boundary Layer. Princeton Univ. Dept. of Aero-
      nautical Engineering. Rep. 249, Jan. 26, 1954.

18. Mossman, Emmet A., Lazzeroni, Frank A., and Pfyl, Frank A.: An
      Experimental Investigation of the Air-Flow Stability of a Scoop-
      Type Normal-Shock Inlet. NACA RM A55A13, 1955.

19. Dryer, Murray, and Beke, Andrew: Performance Characteristics of a
      Normal-Shock Side Inlet Located Downstream of a Canard Control
      Surface at Mach Numbers of 1.5 and 1.8. NACA RM E52F09, 1952.

20. Anderson, Warren E., and Scherrer, Richard: Investigation of a Flow
      Deflector and an Auxiliary Scoop for Improving Off-Design Perform-
      ance of Nose Inlets. NACA RM A54E06, 1954.

21. Mossman, Emmet A., Pfyl, Frank A., and Lazzeroni, Frank A.: Experi-
      mental Investigation at Mach Numbers from 0 to 1.9 of Trapezoidal
      and Circular Side Inlets for a Fighter-Type Airplane. NACA
      RM A55D27, 1955.

22. Mossman, Emmet A., and Anderson, Warren E.: The Effect of Lip Shape
      on a Nose-Inlet Installation at Mach Numbers From 0 to 1.5 and a
      Method for Optimizing Engine-Inlet Combinations. NACA RM A54B08,
      1954.

23. Baughman, L. Eugene, and Gould, Lawrence I.: Investigation of Three
     Types of Supersonic Diffuser Over a Range of Mach Numbers From 1.75
     to 2.74. NACA RM E50L08, 1951.

24. Sears, Richard I., and Merlet, C. F.: Flight Determination of Drag
     and Pressure Recovery of a Nose Inlet of Parabolic Profile at Mach
     Numbers From 0.8 to 1.7. NACA RM L51E02, 1951.

25. Frazer, Alson C., and Anderson, Warren E.: Performance of a Normal-
     Shock Scoop Inlet With Boundary-Layer Control. NACA RM A53D29,
     1953.

26. Davids, Joseph, and Wise, George A.: Investigation at Mach Numbers
     1.5 and 1.7 of Twin-Duct Side Intake System With Two-Dimensional
     6° Compression Ramps Mounted on a Supersonic Airplane. NACA
     RM E53H19, 1953.

27. Obery, Leonard J., and Cubbison, Robert W.: Effectiveness of
     Boundary-Layer Removal Near Throat of Ramp-Type Side Inlet at
     Free-Stream Mach Number of 2.0. NACA RM E54I14, 1954.

28. Obery, L. J., Cubbison, R. W., and Mercer, T. G.: Stabilization Tech-
     niques for Ramp-Type Side Inlets at Supersonic Speeds. NACA
     RM E55A26, 1955.

29. Campbell, Robert C.: Performance of a Supersonic Ramp Inlet With
     Internal Boundary-Layer Scoop. NACA RM E54I01, 1954.

30. Kremzier, Emil J., and Campbell, Robert C.: Angle-of-Attack Super-
     sonic Performance of a Configuration Consisting of a Ramp-Type Scoop
     Inlet Located Either on Top or Bottom of a Body of Revolution.
     NACA RM E54C09, 1954.

31. Piercy, Thomas G., and Johnson, Harry W.: A Comparison of Several
     Systems of Boundary-Layer Removal Ahead of a Typical Conical
     External-Compression Side Inlet at Mach Numbers of 1.88 and 2.93.
     NACA RM E53F16, 1953.

32. Leissler, L. Abbott, and Sterbentz, William H.: Investigation of a
     Translating-Cone Inlet at Mach Numbers From 1.5 to 2.0. NACA
     RM E54B23, 1954.

33. Nettles, J. C., and Leissler, L. A.: Investigation of Adjustable
     Supersonic Inlet in Combination with J34 Engine up to Mach 2.0.
     NACA RM E54H11, 1954.

34. Gorton, Gerald C.: Investigation at Supersonic Speeds of a
     Translating-Spike Inlet Employing a Steep-Lip Cowl. NACA RM E54G29,
     1954.

35. Gorton, Gerald C.: Investigation of Translating-Spike Supersonic
     Inlet as Means of Mass-Flow Control at Mach Numbers of 1.5, 1.8,
     and 2.0. NACA RM E53G10, 1953.

36. Gorton, Gerald C., and Dryer, Murray: Comparison at Supersonic
    Speeds of Translating-Spike Inlets Having Blunt- and Sharp-Lip
    Cowls. NACA RM E54J07, 1955.

37. Piercy, Thomas G., and Johnson, Harry W.: Experimental Investigation
    at Mach Number 1.88, 3.16 and 3.83 of Pressure Drag of Wedge
    Diverters Simulating Boundary-Layer-Removal Systems for Side Inlets.
    NACA RM E53L14b, 1954.

38. Johnson, Harry W., and Piercy, Thomas G.: Effect of Wedge-Type
    Boundary-Layer Diverters on Performance of Half-Conical Side Inlets
    at Mach Number 2.96. NACA RM E54E20, 1954.

39. Fradenburgh, Evan A., and Campbell, Robert C.: Characteristics of a
    Canard-Type Missile Configuration With an Underslung Scoop Inlet at
    Mach Numbers From 1.5 to 2.0. NACA RM E52J22, 1953.

40. Campbell, Robert C., and Kremzier, Emil J.: Performance of Wedge-
    Type Boundary-Layer Diverters for Side Inlets at Supersonic Speeds.
    NACA RM E54C23, 1954.

41. Rolls, L. Stewart: A Flight Comparison of a Submerged Inlet and a
    Scoop Inlet at Transonic Speeds. NACA RM A53A06, 1953.

42. Obery, Leonard J., Stitt, Leonard E., and Wise, George A.: Evalua-
    tion at Supersonic Speeds of Twin-Duct Side-Intake System With Two-
    Dimensional Double-Shock Inlets. NACA RM E54C08, 1954.

43. Obery, Leonard J., and Stitt, Leonard E.: Investigation at Mach
    Numbers 1.5 and 1.7 of Twin-Duct Side Air-Intake System with 9°
    Compression Ramp Including Modifications to Boundary-Layer Removal
    Wedges and Effects of a By-Pass System. NACA RM E53H04, 1953.

44. Goelzer, Fred H., and Cortwright, Edgar M., Jr.: Investigation at
    Mach Number 1.88 of Half of a Conical-Spike Diffuser Mounted as a
    Side Inlet With Boundary-Layer Control. NACA RM E51G06, 1951.

45. McLafferty, George: Theoretical Pressure Recovery Through a Normal
    Shock in a Duct with Initial Boundary Layer. Journal of the Aero-
    nautical Sciences, vol. 20, no. 3, Mar. 1953, pp. 169-174.

46. Fox, Jerome L.: Supersonic Tunnel Investigation by Means of Inclined-
    Plate Technique to Determine Performance of Several Nose Inlets Over
    Mach Number Range of 1.72 to 2.18. NACA RM E50K14, 1951.

47. Howard, Ephraim M., Luciens, Roger W., and Allen, J. L.: Force and
    Pressure Characteristics for a Series of Nose Inlets at Mach Numbers
    From 1.59 to 1.99. V- Analysis and Comparison on Basis of Ram-Jet
    Aircraft Range and Operational Characteristics. NACA RM E51G23,
    1951.

48. Ferri, Antonio, and Nucci, Louis M.: Preliminary Investigation of a
    New Type of Supersonic Inlet. NACA RM L6J31, 1946.

49. Trimpi, Robert L.: An Analysis of Buzzing in Supersonic Ram Jets by
    a Modified One-Dimensional Nonstationary Wave Theory. NACA
    RM L52A18, 1952.

50. Sterbentz, William H., and Evvard, John C.: Criterions for Predic-
    tion and Control of Ram-Jet Flow Pulsations. NACA RM E51C27, 1951.

51. Pearce, R. B.: Causes and Control of Power Plant Surge. Aviation
    Week, vol. 52, no. 3, Jan. 1950, pp. 21-25.

52. Ferri, Antonio, and Nucci, Louis M.: The Origin of Aerodynamic
    Instability of Supersonic Inlets at Subcritical Conditions. NACA
    RM L50K30, 1951.

53. Trimpi, Robert L.: A Theory for Stability and Buzz Pulsation Ampli-
    tude in Ram Jets and an Experimental Investigation Including Scale
    Effects. NACA RM L53G28, 1953.

54. Walker, Curtis L., Sivo, N., and Jansen, Emmert T.: Effect of
    Unequal Air-Flow Distribution from Twin Inlet Ducts on Performance
    of an Axial-Flow Turbojet Engine. NACA RM E54E13, 1954.

55. Goldstein, S.: A Note on the Measurement of Total Head and Static
    Pressure in a Turbulent Stream. Proceedings of the Royal Society
    (London), Ser. A, vol. 155, no. 886, July 1936, pp. 570-575.

56. Rice, S. O.: Mathematical Analysis of Random Noise. Bell System
    Technical Journal, vol. 23, no. 3, July 1944, pp. 282-332.

57. Dryden, Hugh L.: Turbulence Investigations at the National Bureau
    of Standards. Proceedings of the Fifth International Congress of
    Applied Mechanics, Sept. 12-16, 1938, pp. 362-368.

58. Klebanoff, P. S.: Characteristics of Turbulence in a Boundary Layer
    with Zero Pressure Gradient. NACA TN 3178, 1954.

59. Polentz, P. P., Page, W. A., and Levy, L. L., Jr.: The Unsteady
    Normal-Force Characteristics of Selected NACA Profiles at High
    Subsonic Mach Numbers. NACA RM A55C02, 1955.

60. James, Hubert M., Nichols, Nathaniel B., and Phillips, Ralph S.,
    eds.: Theory of Servomechanisms. (M.I.T. Radiation Laboratory
    Series 25) McGraw-Hill Book Co., 1947.

FUSELAGE FLOW CONSIDERATIONS AFFECTING SIDE INLETS

FROM: REF. 1

$M_\infty = 2.0$
$\alpha = 0°$
M_s
$\frac{l}{d} = 3.0$

$\alpha = 0°$

$\alpha \approx 4°$

$\alpha > 9°$
VISCOUS
CROSSFLOW
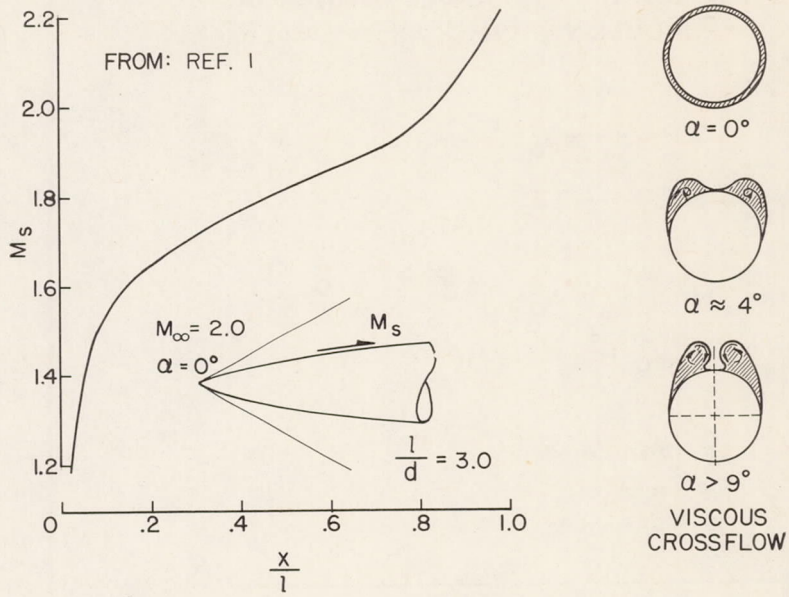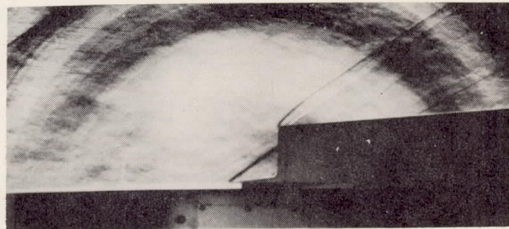
FIGURE 1.

$m_1/m_\infty = $ max.
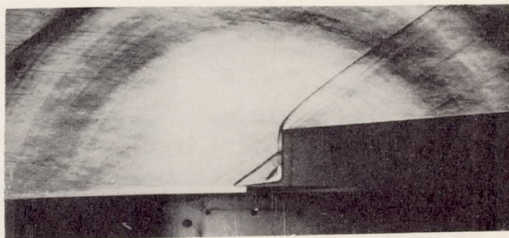
$m_1/m_\infty \approx 0.83$
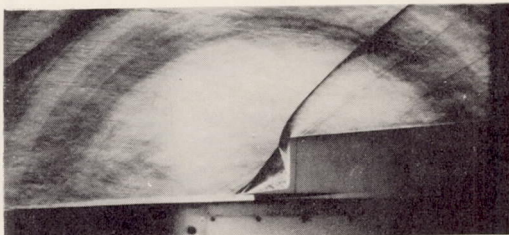
$m_1/m_\infty \approx 0.59$

A-20195

Figure 2.- Extent of flow separation on a ramp in front of an inlet.

SEPARATION PRESSURE RATIO FOR TURBULENT BOUNDARY LAYERS
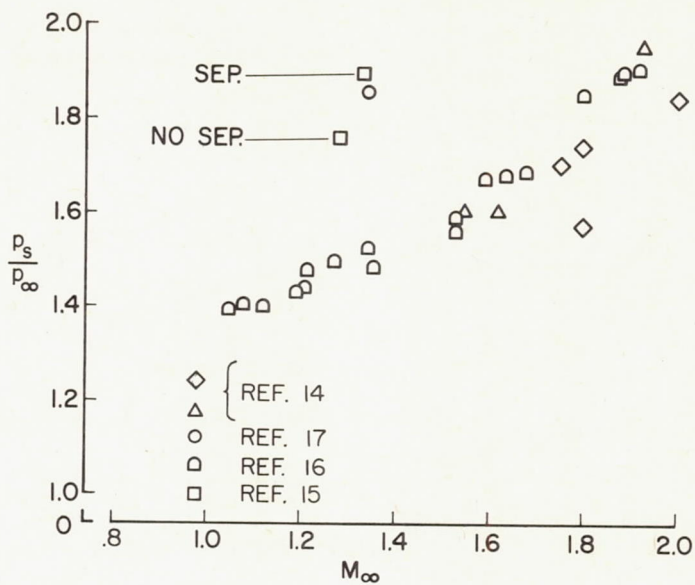
FIGURE 3.

PRESSURE RECOVERY OF NORMAL-SHOCK INLETS
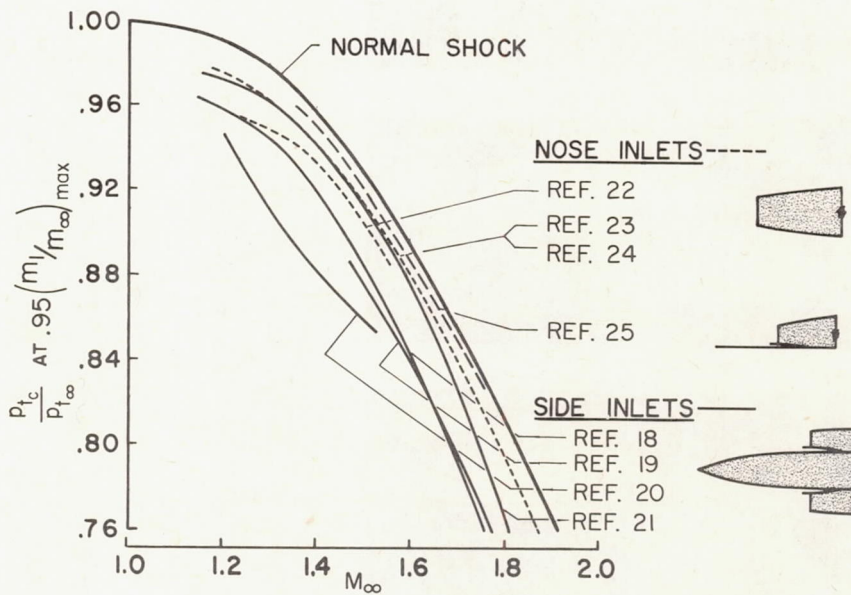
FIGURE 4.

PRESSURE RECOVERY OF OBLIQUE SHOCK SIDE INLETS
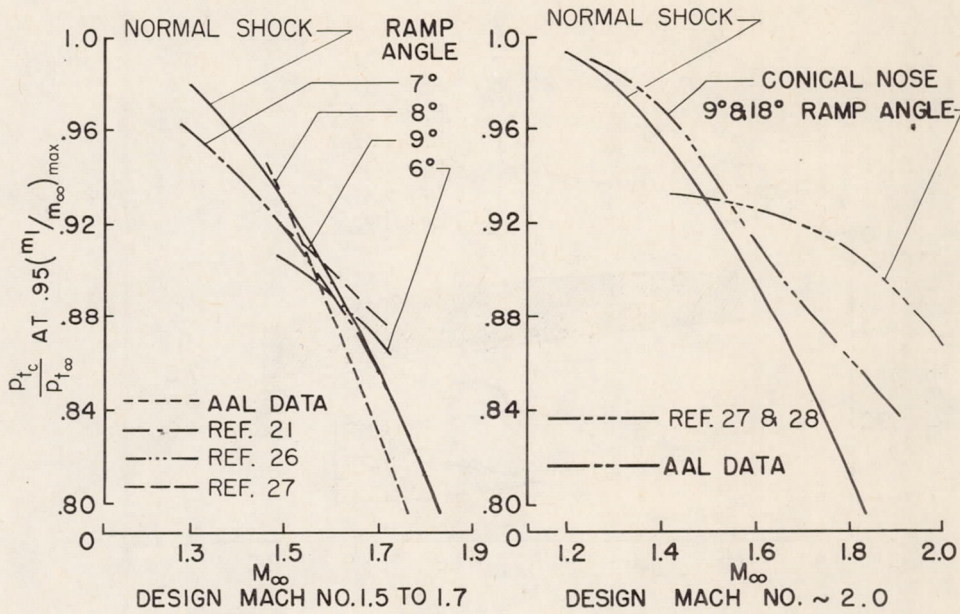
FIGURE 5.

EFFECT OF A FUSELAGE ON THE PRESSURE
RECOVERY OF A 14° RAMP INLET

$$\frac{h}{\delta} = 1.0 \qquad \frac{l}{d} = 7.5$$
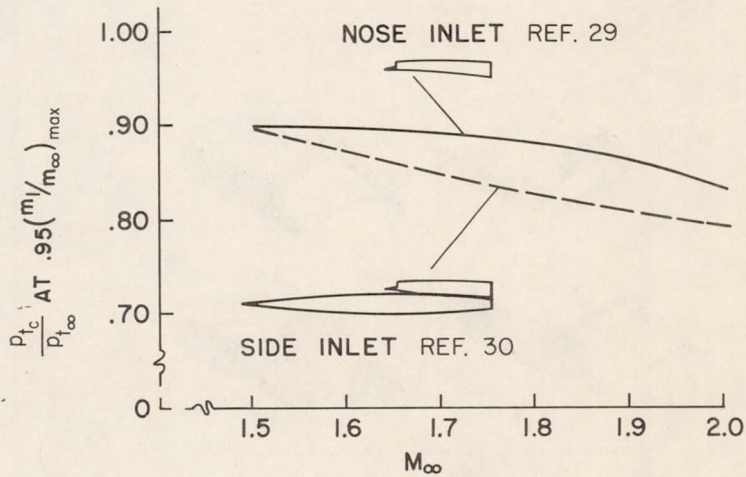
FIGURE 6.

COMPARISON OF CONE INLETS AND HALF-CONE
SIDE INLETS

$M_{DESIGN} = 2.0$ △ REF. 8
—— REF. 9
○ REF. 31
REF. 32
REF. 33
REF. 34
REF. 35
REF. 36
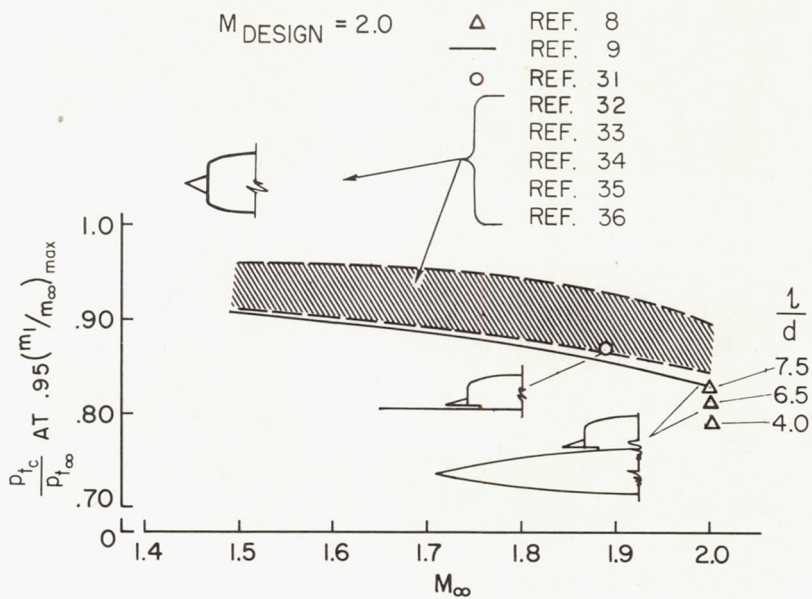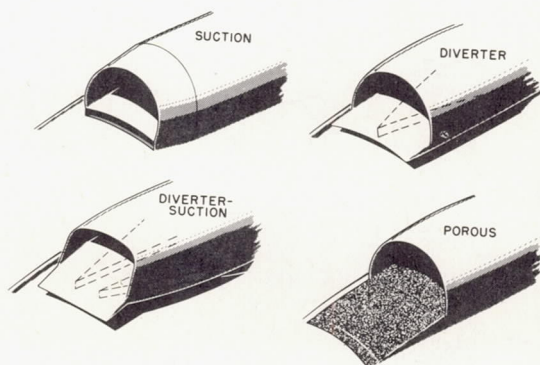
FIGURE 7.

Figure 8.- Boundary-layer control systems for side inlets.
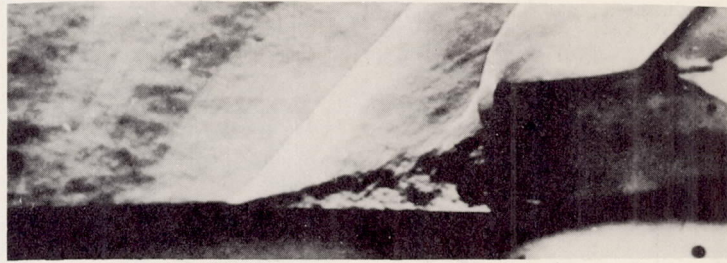
(a) Boundary-layer diverter angle = 130°.
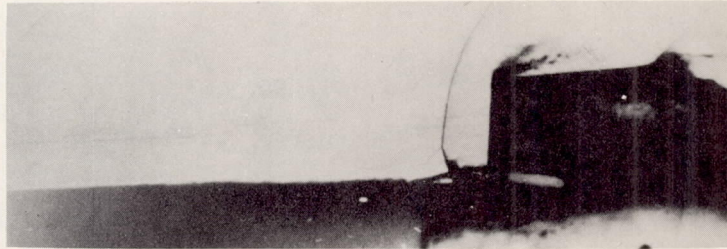
(b) Boundary-layer diverter angle = 65°.

Figure 9.- Effect of a diverter boundary-layer control system.
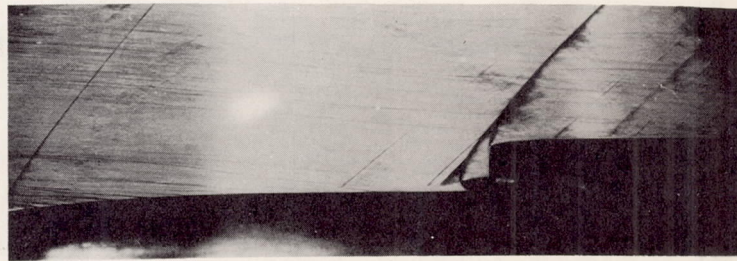
(a) Boundary-layer diverter angle = 40°.
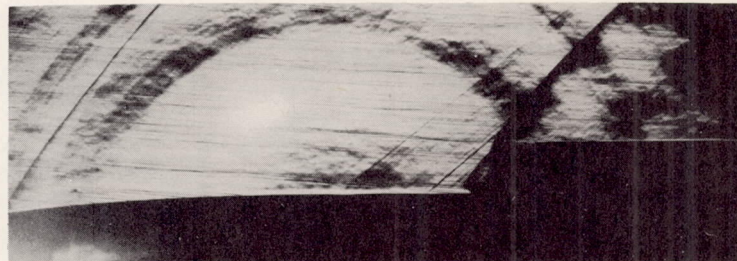
A-20196

(b) Boundary-layer diverter angle = 20°.

Figure 10.- Effect of a diverter-suction boundary-layer control system.

EFFECT OF FUSELAGE BOUNDARY LAYER
ON PRESSURE RECOVERY
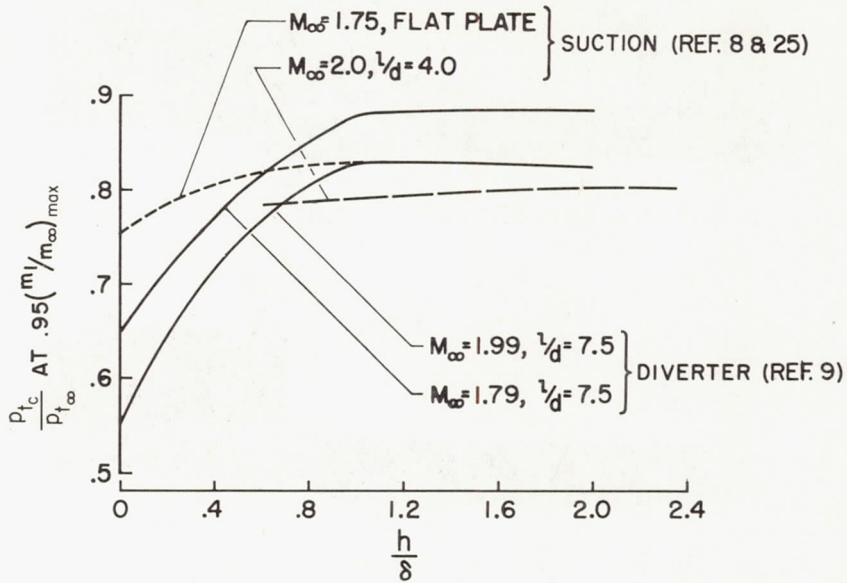
FIGURE 11.

DRAG OF BOUNDARY-LAYER CONTROL SYSTEMS
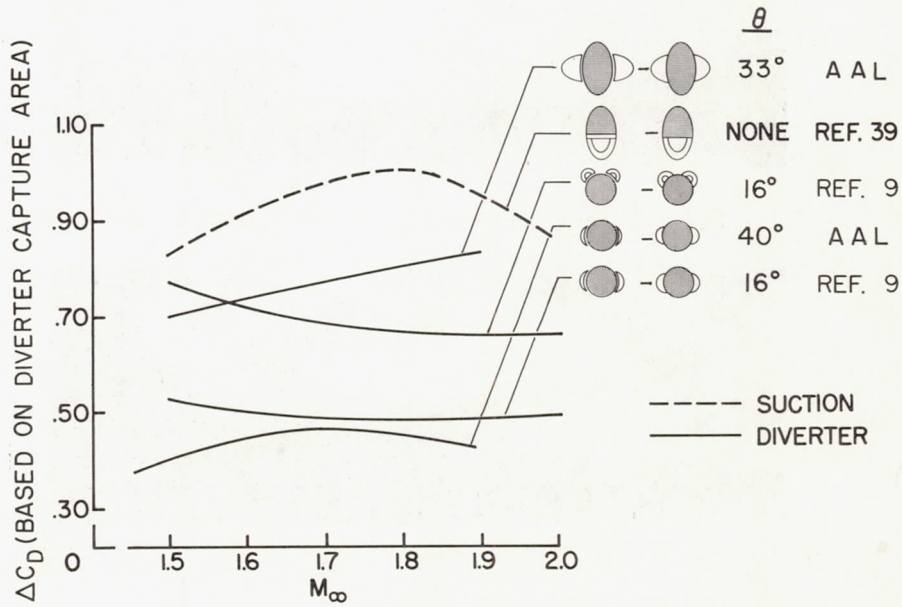
FIGURE 12.

DRAG OF WEDGE DIVERTERS, $\frac{h}{\delta} = 1.0$

(DATA FROM REF. 40)
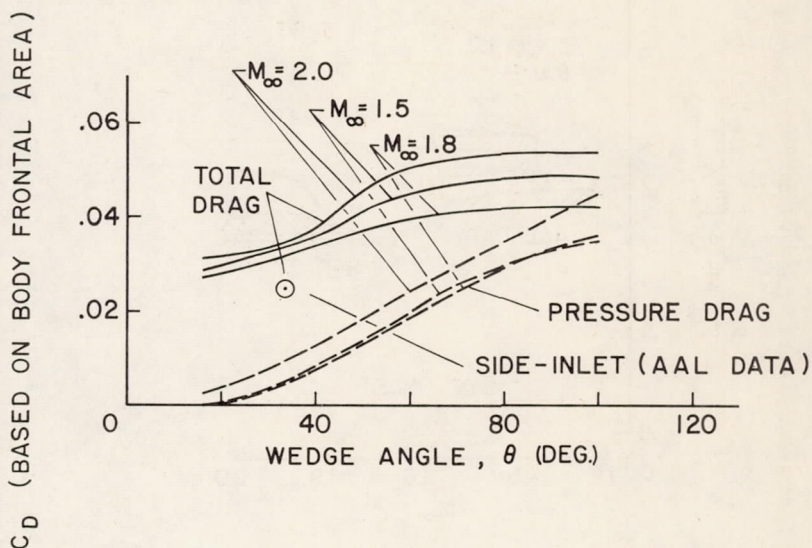
FIGURE 13.

PRESSURE RECOVERY OF BOUNDARY-LAYER
CONTROL SYSTEMS
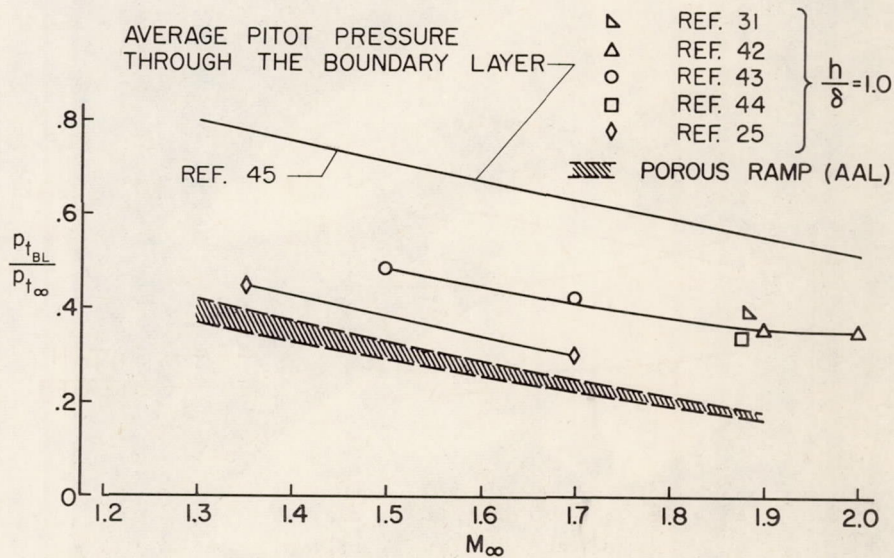
FIGURE 14.

EFFECT OF BOUNDARY-LAYER CONTROL
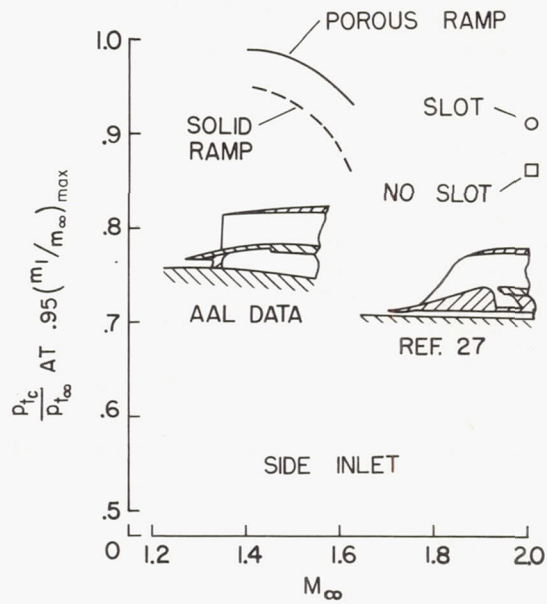
FIGURE 15.
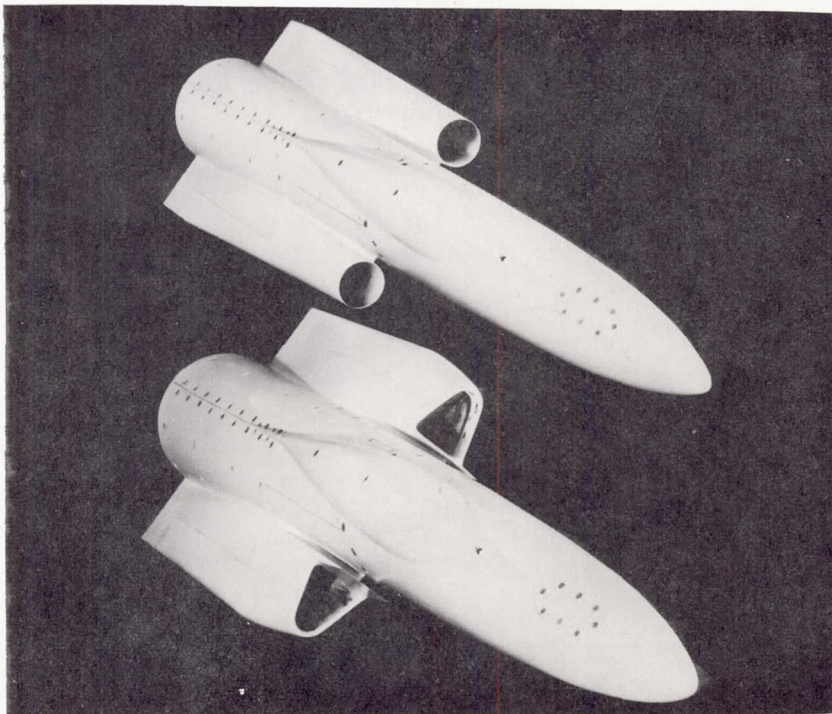
A-20552

Figure 16.- Circular and trapezoidal side inlets.

COMPARISON OF THREE SIDE INLETS ("MATCHED" OPERATION)
35,000 FT ALTITUDE
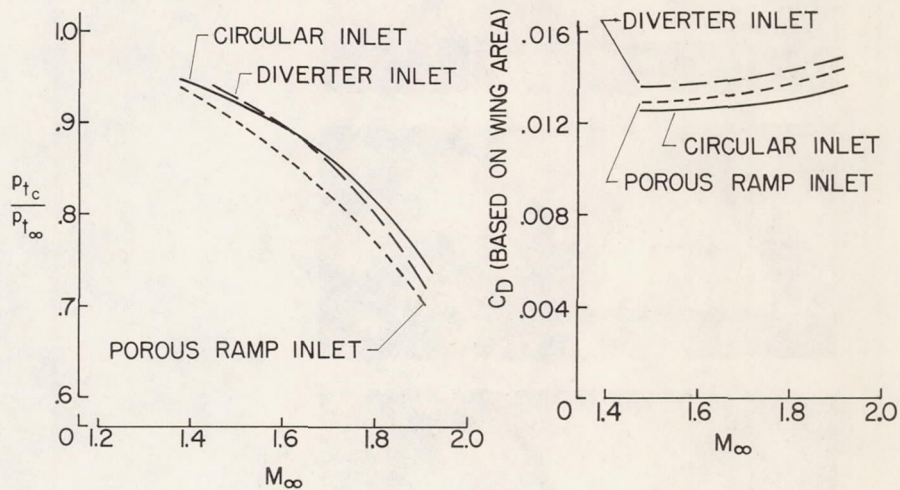
FIGURE 17.
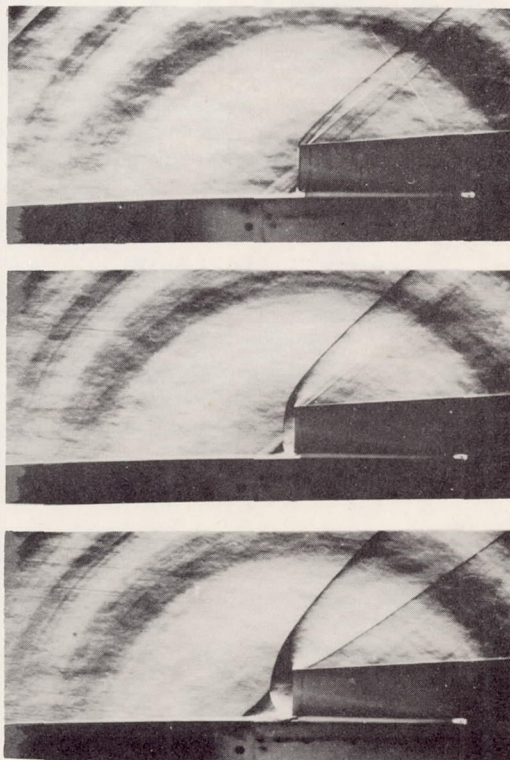
m_1/m_∞ = max.

$m_1/m_\infty \approx 0.9$

$m_1/m_\infty \approx 0.5$

A-19530

Figure 18.- Schlieren photographs of the circular side inlet, M = 1.5.

$m_1/m_\infty = \text{max.}$

$m_1/m_\infty \approx 0.8$

$m_1/m_\infty \approx 0.5$
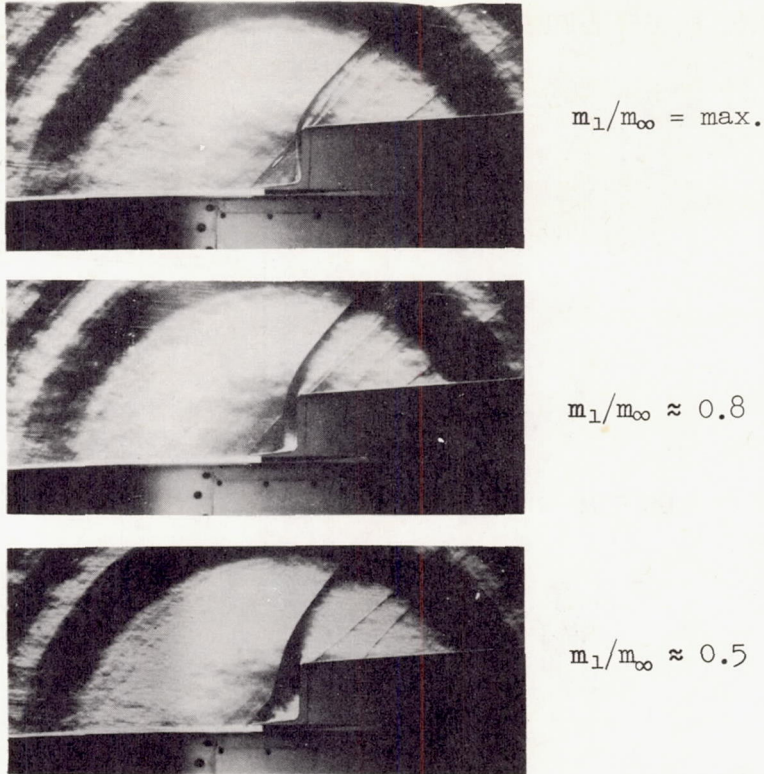
A-19528

Figure 19.- Schlieren photographs of the trapezoidal side inlet, M = 1.5.

NET PROPULSIVE FORCE PARAMETER
35,000 FT ALTITUDE

FIGURE 20.

INTERNAL- COMPRESSION INLET

SECTION A-A
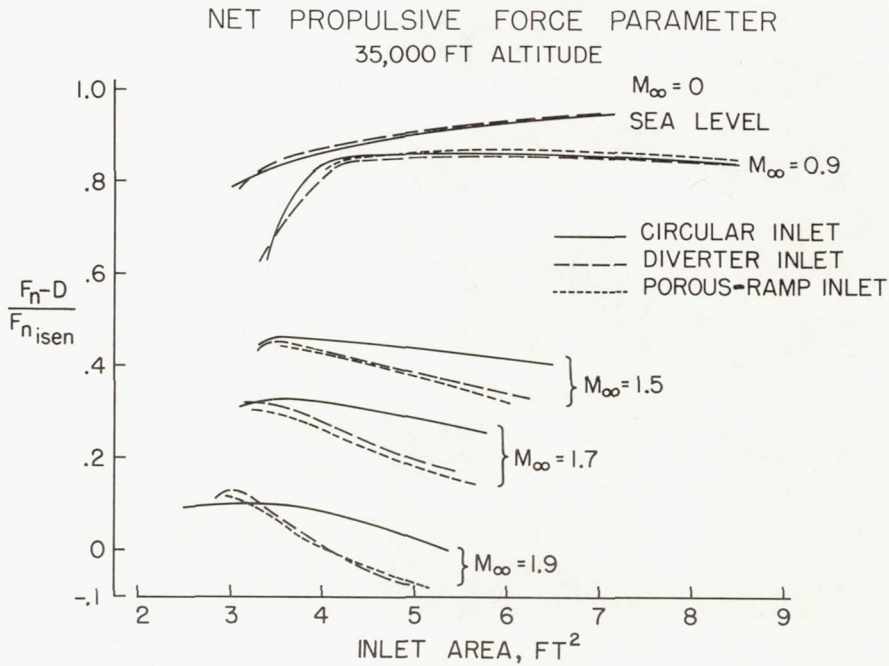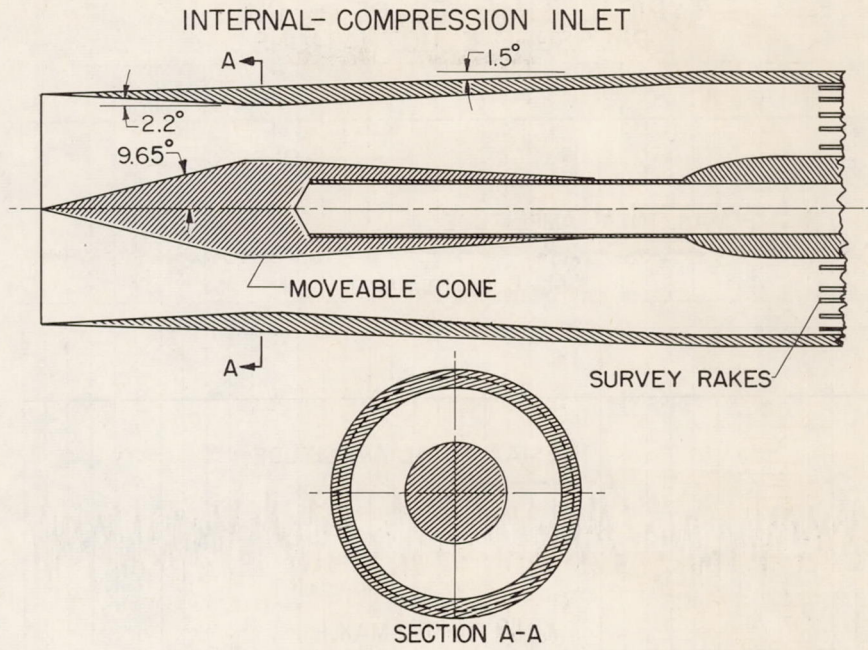
FIGURE 21.

COMPARISON OF CONE INLETS AND AN INTERNAL COMPRESSION INLET

—·— REF. 46 ($\lambda \simeq 10°$)
—··— REF. 47 ($\lambda \simeq 18°$)
— — REF. 36 ($\lambda = 12.5°$)
- - - REF. 48 ($\lambda = 19°$)
—···— REF. 23 ($\lambda = 25°$)

$\frac{p_{t_c}}{p_{t_\infty}}$ AT $\frac{m_1}{m_{\infty \, max}}$ OR .95 $\frac{m_1}{m_{\infty \, max}}$

M_∞
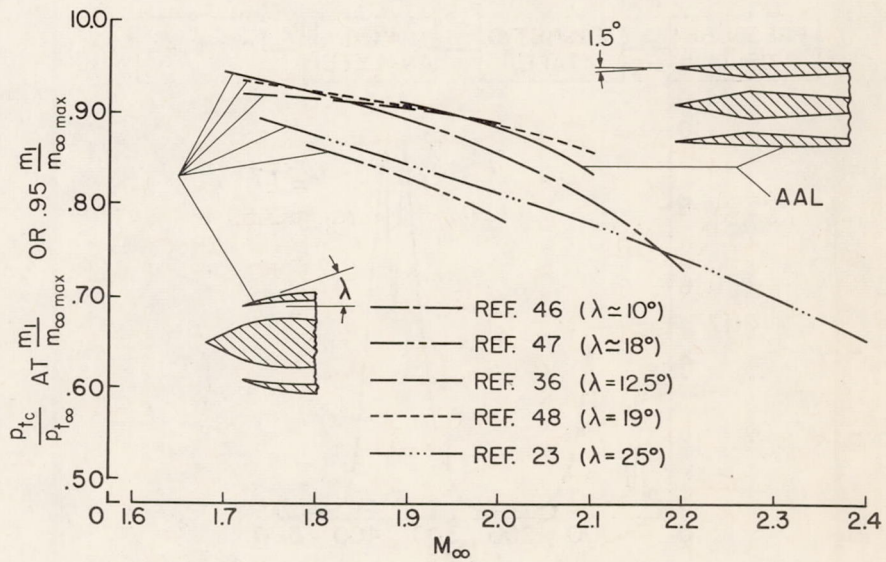
FIGURE 22.

TYPICAL TIME RECORD OF INLET
PRESSURE FLUCTUATIONS
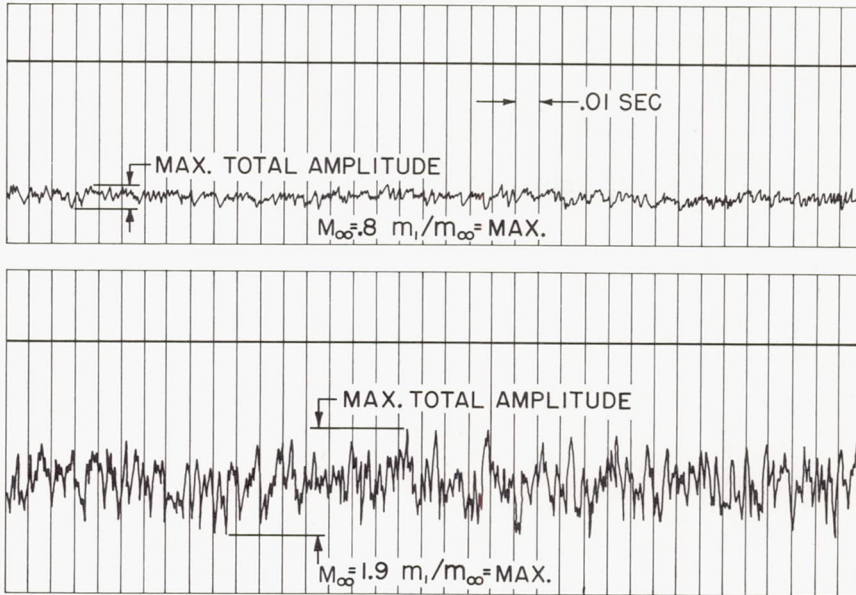
FIGURE 23.

TYPICAL SPECTRAL DISTRIBUTION FOR A
TWIN SIDE INLET
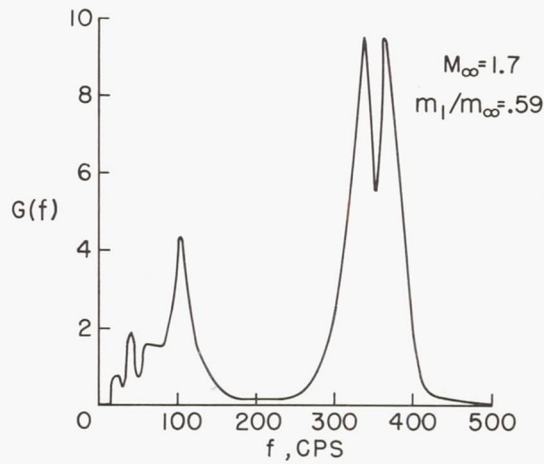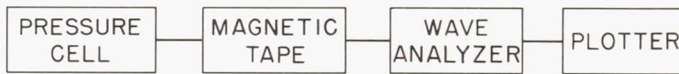
FIGURE 24.

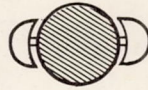## PARAMETERS FOR INLET INSTABILITY

TWIN DUCT
SIDE INLET
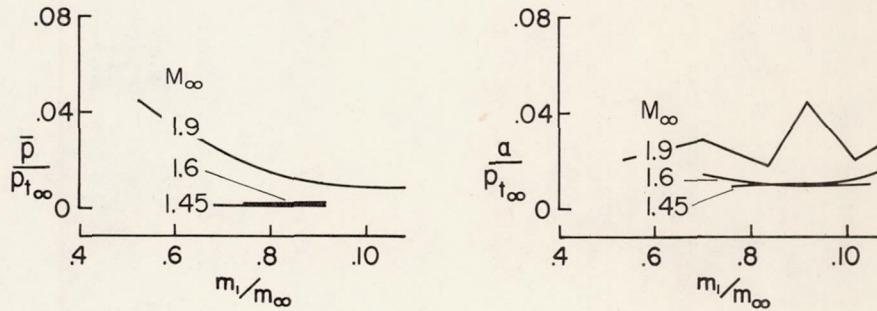
FIGURE 25.
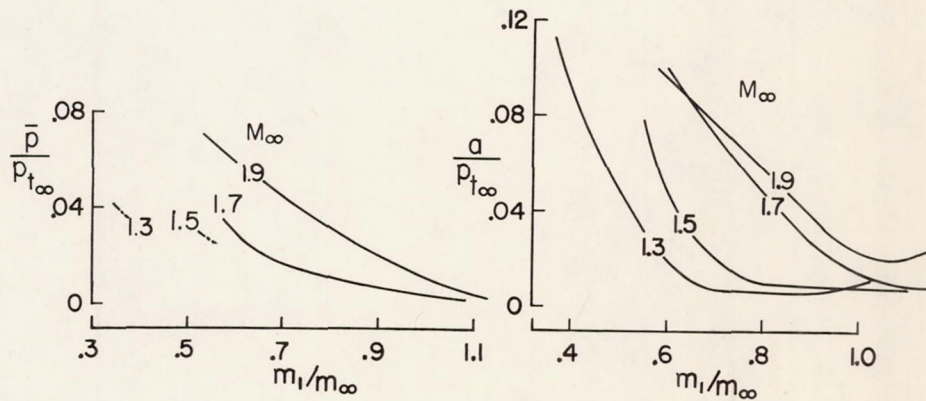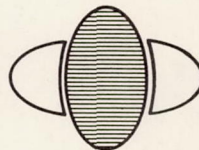
PARAMETERS FOR INLET INSTABILITY

TWIN DUCT
SIDE INLET

FIGURE 26.